Contribution from the University of Windsor, Department of Chemistry and Biochemistry, Windsor, Ontario, Canada N9B 3P4

Study of a Variety of *O*-Methyl, *O*-Ethyl, *O*-Isopropyl, and *O*-*n*-Butyl Dithiocarbonate (Xanthate) Derivatives of Mono-, Di-, and Triphenylgermane. Crystal Structures of $Ph_2Ge[S_2CO(i\text{-}Pr)]_2$ and $Ph_3Ge[S_2COR]$, Where R = Me and *i*-Pr

John E. Drake,* Anil G. Mislankar, and Maria L. Y. Wong

Received October 5, 1990

The *O*-alkyl dithiocarbonate (xanthate) derivatives $PhGe[S_2CO(i\text{-}Pr)]_3$, $Ph_2Ge[S_2CO(i\text{-}Pr)]_2$, $Ph_3Ge[S_2CO(i\text{-}Pr)]$, $Ph_3Ge[S_2COMe]$, $Ph_3Ge[S_2COEt]$, $Ph_3Ge[S_2CO(n\text{-}Bu)]$, $Ph_2Ge[S_2CO(n\text{-}Bu)]_2$, and possibly $PhGe[S_2COR]_3$, where R = Me, and Et, have been prepared in 60–86% yields by reaction of the sodium or potassium salt of the dithiocarbonic (xanthic) acid with trichlorophenyl-, dichlorodiphenyl- or chlorotriphenylgermane. The compounds were characterized by elemental analysis and infrared, Raman and ^1H and ^{13}C NMR spectroscopy. The crystal structures of $Ph_2Ge[S_2CO(i\text{-}Pr)]_2$ and $Ph_3Ge[S_2COR]$, where R = Me and *i*-Pr, were determined. $Ph_2Ge[S_2CO\text{-}i\text{-}Pr]_2$ (**2**), which crystallizes as orthorhombic in space group ($P2_12_12_1$, No. 19), has the cell parameters a = 8.406 (4) Å, b = 14.648 (5) Å, c = 19.551 (6) Å, V = 2407 (2) Å^3, Z = 4, R = 0.0490, and R_w = 0.0501. The environment about germanium is essentially that of a distorted tetrahedron with monodentate xanthate ligands resulting in a S–Ge–S angle of 103.2 (1)° and a C–Ge–C angle of 115.6 (3)°. $Ph_3Ge[S_2CO(iPr)]$ (**3**), which crystallizes as triclinic in space group ($P\bar{1}$, No. 2), has the cell parameters, a = 11.039 (2) Å, b = 11.369 (2) Å, c = 9.299 (2) Å, α = 99.0 (1)°, β = 108.7 (2)°, γ = 99.1 (2)°, V = 1064 (1), Z = 2, R = 0.0576, R_w = 0.0584, and $Ph_3Ge[S_2COMe]$ (**4**), which crystallizes as monoclinic in space group (Cc, No. 9), has the cell parameters a = 16.977 (9) Å, b = 8.510 (1) Å, c = 15.344 (5) Å, β = 118.82 (2)°, V = 1942 (2) Å^3, Z = 4, R = 0.0666, R_w = 0.0658. In both of the Ph_3GeL species, the environment about germanium is again essentially that of a distorted tetrahedron with monodentate ligands resulting in S–Ge–C angles ranging from 98.1 (2) to 112.2 (2)° for **3** and from 98.7 (4) to 114.6° for **4**. The Ge–S bonding distances are 2.251 (3) and 2.252 (3) Å for **2**, 2.270 (2) Å for **3**, and 2.249 Å for **4**. The Ge---O distances in **2** of 3.009 (8) and 2.981 (8) Å are similar to those found for **3**, 3.146 (4) Å, and **4**, 2.98 (1) Å.

Introduction

Despite the extensive and long-term use of *O*-alkyl dithiocarbonates (xanthates) as ligands, particularly toward transition metals,[1,2] structural and spectroscopic characterizations have been more limited with regard to main group elements. We demonstrated recently that the xanthate ligands in $Ph_2Ge[S_2COMe]_2$ are oriented with the oxygen atom rather than the second sulfur atom in the nonbonding position nearest the metal.[3] This is also true of the xanthate ligands in bis(*O*-ethyl xanthato)bis(quinolin-8-olato)tin(IV)[4] but is not true, for example, for the ligands in $Sn(S_2COEt)_2Br_2$.[5] We report on a complete series of phenylgermanes with increasing substitution by the *O*-isopropyl xanthato ligand, which provide further examples of the mode of linkage. A cross section of other xanthate groups was used in attempts to examine the effects of the chain length of the organo groups within the xanthates in terms of mode of linkage and stability, particularly in light of an earlier report on tin compounds that mono- and tris(xanthates) of tin(IV) were difficult to isolate.[5]

Experimental Section

Materials. Chlorotriphenyl-, dichlorodiphenyl-, and trichlorophenylgermane were obtained from Alfa Products. Sodium and potassium *O*-methyl dithiocarbonate, *O*-ethyldithiocarbonate, *O*-isopropyldithiocarbonate and *O*-*n*-butyldithiocarbonate were prepared by adding a slight excess of CS_2 into a mixture of equimolar amounts of NaOH or KOH and ROH, where R = Me, Et, *i*-Pr, and *n*-Bu, in the manner described previously,[6] and their purity was checked by ^1H and ^{13}C NMR spectroscopy. Distilled carbon disulfide (dried over P_4O_{10}) was used as the solvent in all reactions involving a halophenylgermane and a xanthate salt. The reactions were carried out on a vacuum line to exclude air and moisture essentially by using the method described earlier.[3,7]

Typically, the degassed halophenylgermane (approximately 1 mmol) was distilled onto the previously dried and degassed sodium (or potassium) *O*-organo dithiocarbonate (slight excess of 1–3 mmol to ensure complete reaction) held at −196 °C. The solvent, CS_2 (approximately 5 mL), was distilled into the reaction vessel, which was then allowed to warm up slowly toward ambient temperature with stirring. Reactions frequently started well below 0 °C and were cooled occasionally as appropriate to condense the CS_2 being vaporized. After approximately 15 min, the vessel was surrounded by an ice bath, and stirring was continued for 3–4 h. The mixture was then filtered to remove NaCl or KCl and most of the solvent pumped off. The product was then redissolved in fresh CS_2, which was allowed to slowly evaporate at 4 °C to give crystalline compounds. Thus were formed the following complexes. $PhGe[S_2CO(i\text{-}Pr)]_3$ (**1**): yield 65%; mp 75–76 °C. Anal. Calcd for $C_{18}H_{26}O_3S_6Ge$: C, 38.92; H, 4.71. Found: C, 39.45; H, 4.64. $Ph_2Ge[S_2CO(i\text{-}Pr)]_2$ (**2**): yield 77%; mp 123–124 °C. Anal. Calcd for $C_{20}H_{24}O_2S_4Ge$: C, 48.31; H, 4.86. Found: C, 48.46; H, 4.83. $Ph_3Ge[S_2CO(i\text{-}Pr)]$ (**3**): yield 86%; mp 82–85 °C. Anal. Calcd for $C_{22}H_{22}OS_2Ge$: C, 60.17; H, 5.03. Found: C, 60.32; H, 5.10. $Ph_3Ge[S_2COMe]$ (**4**): yield 76%; mp 95–96 °C. Anal. Calcd for $C_{20}H_{18}OS_2Ge$: C, 58.45; H, 4.38. Found: C, 61.68; H, 4.32. $Ph_3Ge[S_2COEt]$ (**5**): yield 70%, mp 73–76 °C. Anal. Calcd for $C_{21}H_{20}OS_2Ge$: C, 59.35; H, 4.70. Found: C, 60.01; H, 4.72. $Ph_3Ge[S_2CO(n\text{-}Bu)]$ (**6**): yield 60%, mp 73–75 °C. Anal. Calcd for $C_{23}H_{24}OS_2Ge$: C, 60.97; H, 5.34. Found: C, 60.91; H, 5.31. $Ph_2Ge[S_2CO(n\text{-}Bu)]_2$ (**7**): yield 65%, mp 49–51 °C. Anal. Calcd for $C_{22}H_{28}O_2S_4Ge$: C, 50.30; H, 5.37; Found: C, 51.75; H, 5.24. $PhGe[S_2COMe]_3$ (**8**): yield 74%, mp 105–107 °C dec. Selected IR and [Raman] data: 1233 vs, $\nu(S_2COC)_a$; 1158 mw, $\nu(S_2COC)_b$; 1054 vvs, $\nu(S_2COC)_c$; [652 (100)], $\nu(S_2COC)_d$; [462 (46)], δ(COC); 430 sh and [431 (10)], $\nu(GeS)_{asym}$; 404 m and [401 (50)], $\nu(GeS)_{sym}$. $PhGe[S_2COEt]_3$ (**9**): yield 75%, mp 60–63 °C dec. Selected IR and [Raman] data: 1237 vvs, $\nu(S_2COC)_a$; 1108 s, $\nu(S_2COC)_b$; 1033 vvs, $\nu(S_2COC)_c$; [682 (26)], $\nu(S_2COC)_d$; 410 m and [408 (40)], $\nu(GeS)_{asym}$; 360 sh and [360 (50)], $\nu(GeS)_{sym}$.

Physical Measurements. The elemental analyses were performed by Guelph Chemical Laboratories, Guelph, Ontario, Canada. The density measurement was performed by the flotation method (C_6H_6/CCl_4). The ^1H and ^{13}C NMR spectra were recorded on a Bruker 300 FT NMR spectrometer in $CDCl_3$ solutions. The infrared spectra were recorded on a Nicolet 5DX FT spectrometer as CsI pellets or Nujol mulls or as neat liquids between CsI plates. The Raman spectra were recorded on a Spectra-Physics 164 spectrometer using the 5145-Å exciting line of an argon ion laser with samples sealed in capillary tubes. The melting points were determined on a Fisher–Johns apparatus.

X-ray Crystallographic Analysis. A prismatic crystal of $Ph_2Ge[S_2CO(i\text{-}Pr)]_2$ (**2**) was sealed in a thin-walled glass capillary and mounted on a Syntex $P2_1$ diffractometer. The X-ray diffraction data were collected by the procedures described elsewhere.[8] The systematic absences ($h00$, $h = 2n + 1$; $0k0$, $k = 2n + 1$; $00l$, $l = 2n + 1$) indicated the space

(1) Burns, R. P.; McCullough, F. P.; McAuliffe, C. A. *Adv. Inorg. Chem. Radiochem.* **1980**, *23*, 211.
(2) Zeiss, W. C. *Acad. R. Sci. (Copenhagen)* **1815**, *1*, 1.
(3) Drake, J. E.; Sarkar, A. B.; Wong, M. L. Y. *Inorg. Chem.* **1990**, *29*, 785.
(4) Raston, C. L.; White, A. H.; Winter, G. *Aust. J. Chem.* **1978**, *31*, 2641.
(5) Gable, R. W.; Raston, C. L.; Rowbottom, G. L.; White, A. H.; Winter, G. *J. Chem. Soc. Dalton Trans.* **1981**, 1392.
(6) Vogel, A. I. *Practical Organic Chemistry*; Longmans, New York, 1956; p 499.
(7) Schmidt, M.; Schumann, H.; Gliniecki, F.; Jaggard, J. F. *J. Organomet. Chem.* **1969**, *17*, 277.
(8) Chadha, R. K.; Drake, J. E.; Sarkar, A. B. *Inorg. Chem.* **1986**, *25*, 2201.

0020-1669/91/1330-2174$02.50/0

Table I. Crystallographic Data for $Ph_2Ge[S_2CO(i\text{-}Pr)]_2$ (**2**), $Ph_3Ge[S_2CO(i\text{-}Pr)]$ (**3**), and $Ph_3Ge[S_2COMe]$ (**4**)

	$Ph_2Ge[S_2CO(i\text{-}Pr)]_2$ (**2**)	$Ph_3Ge[S_2CO(i\text{-}Pr)]$ (**3**)	$Ph_3Ge[S_2COMe]$ (**4**)
chem formula	$C_{20}H_{25}O_2S_4Ge$	$C_{22}H_{22}OS_2Ge$	$C_{20}H_{18}OS_2Ge$
fw	497.24	439.13	411.07
a, Å	8.406 (4)	11.039 (2)	16.977 (9)
b, Å	14.648 (5)	11.369 (2)	8.510 (1)
c, Å	19.551 (6)	9.299 (2)	15.344 (5)
α, deg	90.00	99.0 (1)	90.00
β, deg	90.00	108.7 (2)	118.82 (2)
γ, deg	90.00	99.1 (2)	90.00
V, Å^3	2407 (2)	1064 (1)	1942 (2)
space group	$P2_12_12_1$ (No. 19)	$P\bar{1}$ (No. 2)	Cc (No. 9)
Z	4	2	4
T, °C	24	23	23
λ, Å	0.71069	0.71069	0.71069
ρ_{obsd}, g cm^{-3}	1.35	1.38	1.41
ρ_{calcd}, g cm^{-3}	1.37	1.37	1.41
μ, cm^{-1}	15.55	16.16	17.65
transm factors	0.97–0.99	0.77–1.00	0.88–1.00
R	0.0490	0.0576	0.0666
R_w	0.0510	0.0584	0.0658

group $P2_12_12_1$ (D_2^4, No. 19). The least-squares refinement of the setting angles of 15 reflections in the range $15 < 2\theta < 30°$ led to the cell dimensions given in Table I. During data collection, the intensities of three monitor reflections measured after every 100 reflections decreased by approximately 3–4% and the appropriate scaling factors were applied. The data were corrected for Lorentz and polarization effects, and an empirical absorption correction was applied. A summary of crystal and refinement data is given in Table I.

The position of the germanium atom was obtained from a sharpened Patterson synthesis, and the positions of the remaining non-hydrogen atoms were determined from subsequent difference Fourier maps. The phenyl rings were constrained to a regular hexagon with C–C bond distances of 1.39 Å and C–C–C angles of 120.0°. Phenyl and alkyl hydrogen atoms were also included in their idealized positions with C–H set at 0.95 Å and with isotropic thermal parameters set at 0.01 Å^2 greater than that of the carbon atom to which they were bonded. The data limited the number of atoms treated anisotropically to germanium, sulfur, oxygen, and the carbon atoms of the xanthate groups and those attached to germanium to give convergence at $R = 0.0580$ and $R_w = 0.0586$. During the final stages of the anisotropic full-matrix least-squares refinement, the function $\sum w(|F_o| - |F_c|)^2$ was minimized by using a weighting scheme of the form $w = 1/[\sigma^2(F) + \rho F^2]$. Transforming the x, y, z coordinates of all atoms to $-x$, $-y$, $-z$ produced a significant improvement on the refinement, resulting in convergence at $R = 0.0490$ and $R_w = 0.0501$ based on 170 variables and 1431 unique reflections.

Sources of scattering factors and computer programs used have been given elsewhere.[8] The final atomic coordinates and equivalent isotropic thermal parameters are given in Table II for the non-hydrogen atoms and important distances and bond angles in Table V. Additional crystallographic data are available as supplementary material.

Yellowish block crystals of **3** and **4** were sealed in thin-walled glass capillaries and mounted on a Rigaku AFC6S diffractometer, with graphite monochromated Mo Kα radiation and a 12 kW rotating anode generator.

Cell constants and an orientation matrix for data collection, obtained from a least-squares refinement using the setting angles of 25 carefully centered reflections in the range $26 < 2\theta < 38°$, corresponded to triclinic (for **3**) and monoclinic (for **4**) cells, the dimensions for both being given in Table I. On the basis of the systematic absences of hkl ($h + k \neq 2n$) and $h0l$ ($l \neq 2n$) for **4**, packing considerations, statistical analyses of intensity distributions, and the successful solution and refinement of the structures, the space groups were determined to be $P\bar{1}$ (C_i^1, No. 2) for **3** and Cc (C_s^4, No. 9) for **4**.

The data were collected at a temperature of 23 ± 1° by using the ω–2θ scan technique to a maximum 2θ value of 50.0°. The ω scans of several intense reflections, made prior to data collection, had an average width at half-height of 0.28° (for **3**) and 0.44° (for **4**) with a take-off angle of 6.0°. Scans of $(1.68 + 0.3 \tan\theta)°$, for **3**, and $(1.73 + 0.30 \tan\theta)°$, for **4**, were made at a speed of 32.0°/min (in ω). The weak reflections ($I < 10.0\sigma(I)$) were rescanned (maximum of two rescans), and the counts were accumulated to assure good counting statistics. Stationary background counts were recorded on each side of the reflection. The ratio of peak counting time to background counting time was 2:1. The diameter of the incident beam collimator was 0.5 mm, and the crystal to detector distance was 250.0 mm.

Table II. Final Fractional Coordinates and Isotropic Thermal Parameters for Non-Hydrogen Atoms of $Ph_2Ge[S_2CO(i\text{-}Pr)]_2$ (**2**) with Standard Deviations in Parentheses

atom	x	y	z	U_{eq}, Å$^2 \times 10^3$
Ge	−0.3267 (1)	0.00867 (6)	−0.39415 (5)	41.6 (6)
S1	−0.4785 (3)	−0.0099 (2)	−0.4880 (1)	56 (2)
S2	−0.4112 (4)	−0.0132 (2)	−0.6341 (1)	71 (2)
S3	−0.4998 (4)	0.0628 (2)	−0.3161 (2)	59 (2)
S4	−0.7695 (4)	−0.0193 (3)	−0.2444 (2)	75 (3)
O1	−0.1921 (7)	−0.0086 (5)	−0.5360 (3)	52 (4)
O2	−0.6115 (8)	−0.0952 (4)	−0.3473 (4)	53 (5)
C1	−0.345 (1)	−0.0096 (6)	−0.5566 (5)	46 (6)
C2	−0.064 (1)	0.001 (9)	−0.5872 (5)	60 (8)
C3	−0.040 (2)	0.1008 (8)	−0.6036 (9)	94 (9)
C4	0.077 (1)	−0.044 (1)	−0.5550 (8)	87 (9)
C5	−0.637 (1)	−0.0274 (7)	−0.3028 (5)	46 (6)
C6	−0.709 (1)	−0.1788 (7)	−0.3422 (6)	58 (8)
C7	−0.711 (2)	−0.2185 (8)	−0.4133 (6)	84 (9)
C8	−0.638 (2)	−0.2405 (8)	−0.2896 (7)	92 (9)
C9	−0.1785 (7)	0.1092 (4)	−0.4035 (4)	47 (7)
C10	−0.2323 (7)	0.1952 (4)	−0.4239 (4)	68 (4)
C11	−0.1243 (9)	0.2674 (6)	−0.4318 (5)	80 (4)
C12	0.0374 (9)	0.2530 (6)	−0.4189 (5)	72 (4)
C13	0.0913 (9)	0.1668 (6)	−0.3992 (5)	76 (4)
C14	−0.0168 (9)	0.0951 (6)	−0.3905 (5)	57 (3)
C15	−0.237 (1)	−0.1046 (5)	−0.3626 (3)	42 (7)
C16	−0.215 (1)	−0.1784 (5)	−0.4064 (3)	48 (3)
C17	−0.155 (1)	−0.2606 (5)	−0.3815 (3)	67 (3)
C18	−0.115 (1)	−0.2690 (5)	−0.3125 (3)	68 (4)
C19	−0.136 (1)	−0.1952 (5)	−0.2683 (3)	72 (4)
C20	−0.197 (1)	−0.1130 (5)	−0.2932 (3)	53 (3)

Of the 3956 (for **3**) or 1906 (for **4**) reflections that were collected, 3740 (for **3**) or 1839 (for **4**) were unique ($R_{int} = 0.039$, for **4**). The intensities of three representative reflections that were measured after every 150 reflections remained constant throughout data collection, indicating crystal and electronic stability (no decay correction was applied).

The linear absorption coefficient for Mo Kα is 16.16 (for **3**) and 17.65 cm^{-1} (for **4**). An empirical absorption correction, based on azimuthal scans of several reflections, was applied, which resulted in transmission factors ranging from 0.77 to 1.00 (for **3**) and from 0.88 to 1.00 (for **4**). The data were corrected for Lorentz and polarization effects.

The structures were solved by direct methods.[9] The non-hydrogen atoms other than the carbon atoms of the phenyl rings were refined anisotropically. The final cycles of full-matrix least-squares refinement[10] are based on 2227 (for **3**) or 1048 (for **4**) observed reflections ($I > 3.00\sigma(I)$) and 74 variable parameters for both **3** and **4** and converged (largest parameter shift was 0.0001 times its esd) with unweighted and weighted agreement factors of

$$R = \sum||F_o| - |F_c||/\sum|F_o| = 0.0576 \text{ for } \mathbf{3} \text{ and } 0.0666 \text{ for } \mathbf{4}$$

$$R_w = [(\sum w(|F_o| - |F_c|)^2/\sum wF_o^2)]^{1/2} = 0.0584 \text{ for } \mathbf{3} \text{ and } 0.0658 \text{ for } \mathbf{4}$$

The standard deviation of an observation of unit weight[11] was 1.45 for **3** and 1.85 for **4**. The weighting scheme was based on counting statistics and included a factor ($p = 0.03$) to downweight the intense reflections. Plots of $\sum w(|F_o| - |F_c|)^2$ versus $|F_o|$, reflection order in data collection, $(\sin\theta)/\lambda$, and various classes of indices showed no unusual trends. The maximum and minimum peaks on the final difference Fourier map corresponded to 0.60 and −0.36 (for **3**) and 1.69 and −0.54 e$^-$/Å^3 (for **4**), respectively.

Neutral atom scattering factors were taken from Cromer and Waber.[12] Anomalous dispersion effects were included in F_c;[13] the values for

(9) Structure solution methods: Calbrese, J. C. PHASE—Patterson Heavy Atom Solution Extractor. Ph.D. Thesis, University of Wisconsin-Madison, 1972. Beurskens, P. T. DIRDIF: Direct Methods for Difference Structures—an automatic procedure for phase extension and refinement of difference structure factors. Technical Report 1984/1; Crystallography Laboratory: Toernooiveld, 6525 Ed Nijmegen, Netherlands.

(10) Least-squares: Function minimized: $\sum w(|F_o| - |F_c|)^2$, where $w = 4F_o^2(F_o^2)$, $\sigma^2(F_o^2) = [S^2(C + R^2B) + (pF_o^2)^2]/(Lp)^2$, S = scan rate, C = total integrated peak count, R = ratio of scan time to background counting time, B = total background count, Lp = Lorentz–polarization factor, and p = p factor.

(11) Standard deviation of an observation of unit weight: $[\sum w(|F_o| - |F_c|)^2/(N_o - N_v)]^{1/2}$, where N_o = number of observations and N_v = number of variables.

Table III. Final Fractional Coordinates and B(eq) for Non-Hydrogen Atoms of $Ph_3Ge[S_2CO$*i*-Pr] (3) with Standard Deviations in Parentheses

atom	x	y	z	B(eq), Å^2
Ge1	0.07282 (8)	0.25404 (7)	0.1847 (1)	2.98 (3)
S1	0.0978 (2)	0.4442 (2)	0.3263 (2)	4.27 (8)
S2	0.2674 (2)	0.6837 (2)	0.3883 (3)	5.07 (9)
O	0.3175 (5)	0.4740 (4)	0.2796 (5)	3.5 (2)
C1	0.2395 (7)	0.5360 (6)	0.3285 (7)	3.1 (2)
C2	0.4332 (8)	0.5395 (7)	0.2589 (9)	4.2 (3)
C3	0.5253 (8)	0.4534 (8)	0.273 (1)	5.5 (4)
C4	0.394 (1)	0.5735 (8)	0.104 (1)	6.3 (4)
C5	−0.1159 (4)	0.2012 (5)	0.1242 (6)	4.69 (7)
C6	−0.1919 (5)	0.1453 (5)	−0.0306 (5)	4.69 (7)
C7	−0.3283 (5)	0.1123 (5)	−0.0763 (4)	4.69 (7)
C8	−0.3886 (4)	0.1351 (5)	0.0328 (6)	4.69 (7)
C9	−0.3125 (5)	0.1910 (5)	0.1877 (5)	4.69 (7)
C10	−0.1762 (5)	0.2240 (5)	0.2334 (4)	4.69 (7)
C11	0.1245 (5)	0.2584 (4)	0.0058 (5)	4.22 (7)
C12	0.2068 (5)	0.1838 (4)	−0.0230 (5)	4.22 (7)
C13	0.2416 (5)	0.1822 (4)	−0.1547 (6)	4.22 (7)
C14	0.1941 (5)	0.2552 (4)	−0.2576 (5)	4.22 (7)
C15	0.1118 (5)	0.3298 (4)	−0.2288 (5)	4.22 (7)
C16	0.0770 (5)	0.3314 (4)	−0.0971 (6)	4.22 (7)
C17	0.1664 (4)	0.1571 (4)	0.3168 (5)	3.91 (6)
C18	0.3029 (4)	0.1895 (3)	0.3867 (6)	3.91 (6)
C19	0.3689 (3)	0.1178 (4)	0.4792 (5)	3.91 (6)
C20	0.2985 (4)	0.0135 (4)	0.5019 (5)	3.91 (6)
C21	0.1620 (4)	−0.0190 (3)	0.4321 (6)	3.91 (6)
C22	0.0960 (3)	0.0528 (4)	0.3396 (5)	3.91 (6)

Table IV. Final Fractional Coordinates and B(eq) for Non-Hydrogen Atoms of $Ph_3Ge[S_2COMe]$ (4) with Standard Deviations in Parentheses

atom	x	y	z	B(eq), Å^2
Ge1	0.2792	0.8096 (2)	0.0659	2.83 (5)
S1	0.3905 (3)	0.7018 (6)	0.2044 (4)	4.7 (2)
S2	0.4049 (5)	0.3847 (8)	0.2873 (5)	7.6 (3)
O1	0.2546 (8)	0.540 (1)	0.174 (1)	4.8 (6)
C1	0.344 (1)	0.525 (2)	0.223 (1)	4.5 (8)
C2	0.212 (2)	0.394 (3)	0.175 (2)	8.0 (1)
C3	0.1979 (8)	0.920 (1)	0.100 (1)	5.1 (2)
C4	0.2095 (7)	0.913 (1)	0.1963 (8)	5.1 (2)
C5	0.1504 (8)	0.993 (2)	0.2197 (7)	5.1 (2)
C6	0.0797 (7)	1.080 (1)	0.1468 (9)	5.1 (2)
C7	0.0680 (7)	1.087 (1)	0.0505 (8)	5.1 (2)
C8	0.1271 (9)	1.007 (2)	0.0271 (7)	5.1 (2)
C9	0.3497 (8)	0.953 (1)	0.035 (1)	5.0 (2)
C10	0.3816 (9)	1.090 (2)	0.0916 (9)	5.0 (2)
C11	0.4378 (9)	1.191 (1)	0.0751 (9)	5.0 (2)
C12	0.4621 (8)	1.155 (1)	0.003 (1)	5.0 (2)
C13	0.4302 (9)	1.018 (1)	−0.0536 (9)	5.0 (2)
C14	0.3741 (9)	0.917 (1)	−0.037 (1)	5.0 (2)
C15	0.223 (1)	0.646 (1)	−0.033 (1)	5.4 (2)
C16	0.131 (1)	0.654 (1)	−0.101 (1)	5.4 (2)
C17	0.0904 (7)	0.534 (2)	−0.170 (1)	5.4 (2)
C18	0.141 (1)	0.406 (2)	−0.172 (1)	5.4 (2)
C19	0.2325 (9)	0.397 (2)	−0.104 (1)	5.4 (2)
C20	0.2735 (7)	0.518 (2)	−0.034 (1)	5.4 (2)

$\Delta f'$ and $\Delta f''$ were those of Cromer.[14] All calculations were performed by using the TEXSAN[15] crystallographic software package of Molecular Structure Corp.

The phenyl rings were again constrained to a regular hexagon for **4** because of the amount of data. For **3**, there was sufficient data to go anisotropic on all C atoms with no fixed rings, but in the interest of consistency the rings were similarly fixed on **3** as on **4**. Hydrogen atoms were included in their idealized positions. The final atomic coordinates and equivalent isotropic thermal parameters are given in Tables III and IV for the non-hydrogen atoms and important distances and bond angles in Table VI. Additional crystallographic data are available as supplementary material.

Table V. Interatomic Distances (Å) and Angles (deg) for $Ph_2Ge[S_2CO(i\text{-Pr})]_2$ (2)

Ge–S1	2.251 (3)	Ge–S3	2.252 (3)
Ge–C9	1.939 (7)	Ge–C15	1.927 (6)
S1–C1	1.75 (1)	S3–C5	1.77 (1)
S2–C1	1.61 (1)	S4–C5	1.60 (1)
O1–C1	1.35 (1)	O2–C5	1.34 (1)
O1–C2	1.48 (1)	O2–C6	1.48 (1)
C2–C3	1.51 (2)	C5–C7	1.51 (2)
C2–C4	1.50 (2)	C6–C8	1.49 (2)
Ge···O1	3.009 (8)	Ge···O2	2.981 (8)
Ge···S2	4.755 (3)	Ge···S4	4.753 (4)
S1–Ge–S3	103.2 (1)	C9–Ge–C15	115.6 (3)
S1–Ge–C9	112.3 (2)	S1–Ge–C15	112.3 (2)
S3–Ge–C9	102.2 (2)	S3–Ge–C15	109.9 (2)
Ge–S1–C1	105.2 (3)	Ge–S3–C5	104.8 (3)
S1–C1–S2	119.9 (6)	S3–C5–S4	120.2 (6)
S1–C1–O1	112.4 (7)	S3–C5–O2	110.9 (7)
S2–C1–O1	127.6 (7)	S4–C5–O2	128.9 (8)
C1–O1–C2	119.5 (8)	C5–O2–C6	118.9 (8)
O1–C2–C3	110.0 (1)	O2–C6–C7	105.1 (9)
O1–C2–C4	104.4 (9)	O2–C6–C8	109.4 (7)
C3–C2–C4	114 (1)	C7–C6–C8	114 (1)

Table VI. Interatomic Distances (Å) and Angles (deg) for $Ph_3Ge[S_2CO(i\text{-Pr})]$ (3) and $Ph_3Ge[S_2COMe]$ (4)

$Ph_3Ge[S_2CO(i\text{-Pr})]$ (3)		$Ph_3Ge[S_2COMe]$ (4)	
Ge–S1	2.272 (2)	Ge–S1	2.249 (4)
Ge–C5	1.939 (4)	Ge–C3	1.94 (2)
Ge–C11	1.930 (5)	Ge–C9	1.92 (2)
Ge–C17	1.941 (5)	Ge–C15	1.94 (1)
S1–C1	1.729 (8)	S1–C1	1.78 (2)
S2–C1	1.629 (7)	S2–C1	1.57 (2)
O–C1	1.34 (1)	O–C1	1.34 (2)
O–C2	1.46 (1)	O–C2	1.44 (3)
C2–C3	1.51 (1)		
C2–C4	1.50 (1)		
Ge···O	3.155 (4)	Ge···O	2.98 (1)
Ge···S2	4.815 (2)	Ge···S2	4.71 (1)
S1–Ge–C5	98.1 (2)	S1–Ge–S3	109.1 (4)
S1–Ge–C11	112.2 (2)	S1–Ge–C9	98.7 (4)
S1–Ge–C17	110.2 (1)	S1–Ge–C15	108.6 (4)
C5–Ge–C11	111.6 (2)	C3–Ge–C9	111.5 (6)
C5–Ge–C17	112.2 (2)	C3–Ge–C15	114.6 (6)
C11–Ge–C17	111.8 (2)	C9–Ge–C15	113.2 (2)
Ge–S1–C1	108.4 (3)	Ge–S1–C1	105.3 (6)
S1–C1–S2	119.7 (5)	S1–C1–S2	122 (1)
S1–C1–O	113.9 (5)	S1–C1–O	107 (1)
S2–C1–O	126.4 (5)	S2–C1–O	130 (2)
C1–O–C2	120.0 (5)	C1–O–C2	111 (1)
O–C2–C3	105.5 (6)		
O–C2–C4	109.5 (6)		
C3–C2–C4	112.7 (8)		

Results and Discussion

The synthesis of tris(*O*-isopropyl dithiocarbonato)phenylgermane, bis(*O*-isopropyl dithiocarbonato)diphenylgermane, and (*O*-isopropyl dithiocarbonato)triphenylgermane is readily achieved in 65–86% yield by the action of the appropriate sodium or potassium salt with trichlorophenyl-, dichlorodiphenyl-, or chlorotriphenylgermane in CS_2 as solvent in accord with the general equation

$$Ph_{4-n}GeCl_n + nNaS_2CO(i\text{-Pr}) \rightarrow Ph_{4-n}Ge[S_2CO(i\text{-Pr})]_n + nNaCl$$

$$n = 1, 2, 3$$

The corresponding reactions to produce (*O*-methyl dithiocarbonato)-, (*O*-ethyl dithiocarbonato)- and (*O*-*n*-butyl dithiocarbonato)triphenylgermane and bis(*n*-butyl dithiocarbonato)diphenylgermane in yields of 76, 70, 60, and 65%, respectively,

(12) Cromer, D. T.; Waber, J. T. *International Tables for X-ray Crystallography*; The Kynoch Press, Birmingham, England, 1974; Vol. IV, Table 2.2 A 1974.
(13) Ibers, J. A.; Hamilton, W. C. *Acta Crystallogr.* **1964**, *17*, 781.
(14) Cromer, D. T. *International Tables for X-ray Crystallography*; The Kynoch Press: Birmingham, England, 1974; Table 2.3.1.
(15) TEXSAN—TEXRAY Structure Analysis Package. Molecular Structure Corp., 1985.

Table VII. ^{1}H NMR Chemical Shifts for Compounds **1–9**[a,b] with those of $Ph_2Ge[S_2COMe]_2$ and $Ph_2Ge[S_2COEt]_2$ Added for Comparison[c]

no.	compd	Ge–C_6H_5	$OCH_3/OCH_2/OCH$	CCH_3'/CCH_2'	$J_{HH'}$, Hz
1	$PhGe[S_2CO(i\text{-}Pr)]_3$	7.71–7.74, 7.44–7.47 (5 H)	5.53 (3 H, sept)	1.22 (18 H, d)	6.2
2	$Ph_2Ge[S_2CO(i\text{-}Pr)]_2$	7.72–7.75, 7.43–7.45 (10 H)	5.36 (2 H, sept)	0.91 (12 H, d)	6.0
3	$Ph_3Ge[S_2CO(i\text{-}Pr)]$	7.60–7.64, 7.36–7.46 (15 H)	5.41 (1 H, sept)	0.78 (6 H, d)	6.0
4	$Ph_3Ge[S_2COMe]$	7.59–7.64, 7.40–7.47 (15 H)	3.72 (3 H, s)		
5	$Ph_3Ge[S_2COEt]$	7.58–7.62, 7.37–7.43 (15 H)	4.24 (2 H, q)	0.77 (3 H, t)	7.2
6	$Ph_3Ge[S_2CO(n\text{-}Bu)]$	7.59–7.62, 7.36–7.44 (15 H)	4.20 (2 H, t)[d]	0.89 (2 H, m)	6.7
7	$Ph_2Ge[S_2CO(n\text{-}Bu)]_2$	7.72–7.75, 7.41–7.49 (10 H)	4.22 (4 H, t)[e]	1.05 (4 H, m)	6.0
8	$PhGe[S_2COMe]_3$	7.69–7.71, 7.45–7.47 (5 H)	3.96 (9 H, s)		
9	$PhGe[S_2COEt]_3$	7.71–7.74, 7.44–7.47 (5 H)	4.45 (6 H, q)	1.23 (9 H)	6.8
	$Ph_2Ge[S_2COEt]_2$	7.72–7.75, 7.37–7.43 (10 H)	4.28 (4 H, q)	0.97 (6 H, t)	
	$Ph_2Ge[S_2COMe]_2$	7.72–7.75, 7.36–7.46 (10 H)	3.79 (6 H, s)		

[a] The spectra were recorded in $CDCl_3$ and reported in ppm from Me_4Si, using $CHCl_3$ as a second standard. [b] Number of protons and multiplicities are in parentheses (s = singlet, q = quartet, t = triplet, m = multiplet, and sept = septet). [c] See reference 3. [d] Multiplet and a triplet corresponding to $O\text{–}CH_2CH_2''CH_3'''$ are seen centered at 1.26 and 0.73 ppm, with $J_{H''H'''}$ = 7.2 Hz. [e] A multiplet and a triplet corresponding to $O\text{–}CH_2CH_2''CH_3'''$ are seen centered at 1.31 and 0.65 ppm, with $J_{H''H'''}$ = 7.3 Hz.

Table VIII. ^{13}C NMR Chemical Shifts for Compounds **1–9**[a] with Those of $Ph_2Ge[S_2COEt]_2$ and $Ph_2Ge[S_2COMe]_2$ Added for Comparison[b,c]

		Ge–C_6H_5						
no.	compd	C(1)	C(2,6)	C(4)	C(3,5)	$OCH_3/OCH_2/OCH$	$OCCH_3/OCCH_2$	CS_2
1	$PhGe[S_2CO(i\text{-}Pr)]_3$	135.87	132.99	131.37	128.87	80.47	20.85	207.04
2	$Ph_2Ge[S_2CO(i\text{-}Pr)]_2$	134.73	133.70	130.75	128.78	79.78	20.47	209.25
3	$Ph_3Ge[S_2CO(i\text{-}Pr)]$	134.47	134.47	130.00	128.53	78.99	20.28	211.18
4	$Ph_3Ge[S_2COMe]$	134.43	134.43	130.03	128.55	59.99		212.65
5	$Ph_3Ge[S_2COEt]$	134.47	134.47	130.03	128.57	70.52	12.85	211.93
6	$Ph_3Ge[S_2CO(n\text{-}Bu)]$	134.45	134.45	130.01	128.57	74.70	29.47[d]	212.22
7	$Ph_2Ge[S_2CO(n\text{-}Bu)]_2$	134.08	133.65	130.73	128.75	75.02	29.59[e]	210.38
8	$PhGe[S_2COMe]_3$	*f*	132.49	131.33	128.92	60.79		208.76
9	$PhGe[S_2COEt]_3$	*f*	132.75	131.34	128.88	71.60	13.34	207.87
	$Ph_2Ge[S_2COEt]_2$	134.15	133.64	130.75	128.78	69.94	13.07	210.11
	$Ph_2Ge[S_2COMe]_2$	133.81	133.65	130.59	128.78	60.34		211.05

[a] The spectra were recorded in $CDCl_3$ and reported in ppm from Me_4Si. [b] See reference 3. [c] In the D_2O solution spectrum of the $KS_2CO(i\text{-}Pr)$ salt, peaks are seen at 21.59, 78.80 and 232.82 ppm, and for $KS_2CO(n\text{-}Bu)$ at 13.91, 19.56, 31.00 and 75.16 ppm. For the corresponding NaS_2COEt and NaS_2COMe solutions, the peaks are at 14.67, 71.28 and 233.71 ppm and 60.75 and 233.12 ppm respectively. [d] CH_2CH_2 chemical shifts are at 18.67 and 13.52 ppm. [e] CH_2CH_2 chemical shifts are at 18.76 and 13.52 ppm. [f] Not observed.

for $Ph_3Ge[S_2COMe]$, $Ph_3Ge[S_2COEt]$, $Ph_3Ge[S_2CO(n\text{-}Bu)]$, and $Ph_2Ge[S_2CO(n\text{-}Bu)]_2$ were carried out similarly by using the appropriate dithiocarbonate salt. We were not able to obtain analyses for samples of $PhGe[S_2COMe]_3$ and $PhGe[S_2COEt]_3$ because they decomposed too rapidly, although we were able to obtain sharp melting points before they decomposed, suggesting that the spectra recorded immediately were authentic. It is interesting to note that while attempts to prepare $Cl_2Sn[S_2COR]_2$, R = Me and Et, were successful, the mono and tris compounds were not obtained.[5]

The compounds (**1–7**), which are only susceptible to moisture and air on long exposure, are colorless solids that readily dissolve in chloroform, which was therefore used as the preferred solvent for recording NMR spectra. Compounds **8** and **9** decomposed over a period of ca. 8 h when separated from solution.

NMR Spectra. The ^{1}H and ^{13}C{H} NMR spectra data are presented in Tables VII and VIII. The ^{1}H NMR spectra confirm that the products are over 98% pure relative to any hydrogen-containing impurities, and integrations are as predicted for compounds **1–7**. The signals due to the phenyl groups are similar in all species and are comparable to other phenylgermanium derivatives containing Ge–S bonds.[16-18] The xanthate ligands give the expected first-order spectra, except of course for the two CH_2 groups of the *n*-butyl group, with chemical shifts comparable to those of the bis derivatives[3] or salts. The chemical shifts for the hydrogen atoms on the carbon attached to oxygen (i.e. $OCH_3/OCH_2/OCH$) are similar for a given ligand regardless of whether the phenylgermane has one, two, or three xanthate groups attached to germanium. By contrast, the CCH_3 chemical shifts are essentially the same for *O*-isopropyl and *O*-ethyl derivatives, provided the number of xanthate groups is the same, but increase regularly as the number of xanthate groups increases as do the OCH_2CH_2 chemical shifts with an increase in the number of *O*-*n*-butyl dithiocarbonate groups attached.

In the ^{13}C NMR spectra, four sets of peaks are observed that are assignable to CS_2, Ge–C_6H_5, $OCH_3/OCH_2/OCH$, and $OCCH_3/CH_2$, with two additional peaks for the *n*-butyl derivatives. The chemical shifts of the ligand methyl, ethyl, iso-propyl, and *n*-butyl carbon resonances are relatively unaltered by a change in the number of ligands and are also similar to those of the corresponding salts even though the latter had to be dissolved in D_2O. However, the chemical shifts of the dithiocarbonate carbon resonances of the germanium compounds are considerably shifted relative to those of the sodium salts. This is to be expected as the environment about the CS_2 carbon is presumably the most affected by the formation of one strong S–Ge covalent bond. Finally, the chemical shifts of the phenyl groups are dependent on the number of xanthate groups rather than their nature.

Infrared and Raman Spectra. Six prominent features in the infrared spectra, which fall into three sets of pairs of similar intensities, act as particularly useful fingerprints for phenyl groups attached to germanium. These, in decreasing order of intensity, are consistently seen close to 739 and 696 cm^{-1}, 462 and 336 cm^{-1}, and finally 1434 and 1096 cm^{-1}. The assignments of these modes in Tables IX and X are in accord with the generally accepted Whiffen notation[19] and the relative intensities of these peaks are consistent with the total number of phenyl groups attached to germanium. In the Raman effect the presence of the phenyl group is typified by an intense peak close to 1000 cm^{-1} with weaker features at approximately 1589, 1180, 1155, 1085, 1025, and 680 cm^{-1} in regions associated with the S_2COC stretching mode.

(16) Chadha, R. K.; Drake, J. E.; Sarkar, A. B. *Inorg. Chem.* **1985**, *24*, 3156.
(17) Chadha, R. K.; Drake, J. E.; Sarkar, A. B. *J. Organomet. Chem.* **1987**, *323*, 271.
(18) Chadha, R. K.; Drake, J. E.; Sarkar, A. B. *Inorg. Chim. Acta* **1988**, *143*, 31.
(19) Whiffen, D. H. *J. Chem. Soc.* **1956**, 1350.

Table IX. Selected Features and Their Assignments in the Vibrational Spectra of Compounds **1–3**[a,b]

$Ph_3Ge[S_2CO(i\text{-}Pr)]_3$ (**1**)		$Ph_2Ge[S_2CO(i\text{-}Pr)]_2$ (**2**)		$Ph_3Ge[S_2CO(i\text{-}Pr)]$ (**3**)		
IR[c]	Raman[d]	IR[c]	Raman[d]	IR[c]	Raman[d]	assgnts
g	1576 (8)	*g*	1581 (22)	*g*	1581 (23)	*l*-phenyl
1440 w	*g*	1440 mw	1443 (5)	1430 m	1430 (4)	*n*-phenyl
1248 vvs	1245 (1)	1235 vvs	1234 (5)	1231 vs	1230 (1)	$\nu(S_2COC)_a$[e]
1180 vw	1180 (2)	1180 wsh	1182 (9)	1180 w	1182 (7)	*a*-phenyl
1144 w	1156 (3)	1150 w	1155 (9)	1150 w	1155 (7)	*e*-phenyl
1086 vs	1082 (3)	1085 vs	1086 (7)	1091 vs	1086 (7)	$\nu((S_2COC)_b$[e] and *q*-phenyl[f]
1025 vvs	1033 (100)	1029 vvs	1033 (80)	1032 vs	1030 (35)	$\nu(S_2COC)_c$[e]
g	*g*	*g*	1024 (20)	*g*	1021 (20)	*b*-phenyl
g	994 (71)	*g*	996 (100)	1000 sh	996 (100)	*p*-phenyl
732 mw	*g*	737 ms	739 (1)	738 s	741 (1)	*f*-phenyl
691 mw	*g*	698 ms	*g*	698 s	*g*	*v*-phenyl
	691 (65)		690 (53)		689 (13)	$\nu(S_2COC)_d$[e]
667 vw sh	672 (17)	667 w sh	670 (15)	670 w	664 (10)	*r*-phenyl[f]
	470 (8)		468 (10)		470 (4)	*y*-phenyl[f] and δCOC
454 mww		459 ms br		462 ms		
	451 (23)		447 (12)		450 (5)	
410 w	408 (46)	420 ms	419 (20)	414 mw	412 (12)	$\nu(Ge\text{–}S)_{asym}$
373 w	374 (56)	376 w	375 (37)			$\nu(Ge\text{–}S)_{sym}$
338 w	334 (21)	332 ms	*g*	332 m	*g*	*t*-phenyl[f]

[a] Parentheses denote relative intensities in the Raman effect. [b] s = strong, m = medium, w = weak, sh = shoulder, br = broad, and v = very. [c] Run as CsI pellets. [d] Run as a solid in a glass capillary. [e] In the corresponding salt these appear at 1131, 1084, 1056, and 662 cm^{-1}. [f] X-sensitive modes. [g] Not observed.

Table X. Selected Features and Their Assignments in the Vibrational Spectra of Compounds **4–7**[a,b]

$Ph_3Ge[S_2COMe]$ (**4**)		$Ph_3Ge[S_2COEt]$ (**5**)		$Ph_3Ge[S_2CO(n\text{-}Bu)]$ (**6**)		$Ph_2Ge[S_2CO(n\text{-}Bu)]_2$ (**7**)		
IR[c]	Raman[d]	IR[c]	Raman[d]	IR[e]	Raman[d]	IR[c]	Raman[d]	assgnts
g	1584 (26)	*g*	1582 (23)	*g*	1583 (26)	*g*	1582 (20)	*l*-phenyl
1435 s	1432 (2)	1435 ms	*g*	1434 ms	1430 (2)	1433 ms	*g*	*n*-phenyl
1234 vs	*g*	1217 vs		1205 s	*g*	1222 s	*g*	$\nu(S_2COC)_a$[e]
1187 sh	1185 (10)	1180 w sh	1185 (6)	*g*	1185 (7)	*g*	1184 (4)	*a*-phenyl
1165 sh	1160 (6)	1140 sh	1155 (6)	1160 sh	1156 (5)	1155 sh	1155 (10)	*e*-phenyl
1158 ms	*g*	1115 m	1120 (2)	1149 mw	*g*	1132 m	1122 (2)	$\nu(S_2COC)_b$[e]
1093 s	1088 (7)	1092 ms	1087 (7)	1092 ms	1089 (5)	1090 m	1086 (4)	*q*-phenyl[f]
1059 vs	1058 (15)	1044 vs	1041 (23)	1048 vs	1048 (26)	1041 vs	1043 (50)	$\nu(S_2COC)_c$[e]
1024 mw	1026 (15)	*g*	1024 (17)	*g*	1025 (15)	*g*	1026 (12)	*b*-phenyl
1000 sh	1000 (100)	1000 m	996 (100)	1000 sh	1000 (100)	1000 wsh	998 (100)	*p*-phenyl
739 s	*g*	739 s	*g*	738 s	741 (1)	737 ms	*g*	*f*-phenyl
698 s	*g*	698 s	*g*	698 s	*g*	698 ms	*g*	*v*-phenyl
g	647 (19)	*g*	690 (8)	*g*	642 (12)	*g*	691 (2)	$\nu(S_2COC)_d$[d]
	668 (17)	674 w	665 (14)	679 w	667 (17)	667 sh	672 (15)	r-phenyl[f]
	472 (10)							*y*-phenyl and δ(COC)
466 s br	451 (3)	464 s br	460 (1)	462 s br	460 (2)	460 ms br	460 (2)	
411 mW	408 (11)	427 m br	417 (6)	414 m br	412 (12)	418 m br	420 (14)	$\nu(Ge\text{–}S)_{asym}$
						g	411 (25)	$\nu(Ge\text{–}S)_{sym}$
336 s	*g*	331 s	328 (2)	332 ms	*g*	323 m	*g*	*t*-phenyl

[a] Parentheses denote relative intensities in the Raman effect. [b] s = strong, m = medium, w = weak, sh = shoulder, br = broad, and v = very. [c] Run as CsI pellets. [d] Run as a solid in a glass capillary. [e] In the corresponding *n*-butyl xanthate salt these appear at 1150, 1108, 1071, and 698 cm^{-1}. [f] X-sensitive modes. [g] Not observed.

In an earlier paper,[3] we referred to the many, by and large ambiguous, studies that have attempted to make specific assignments to the C–O and C–S vibrations of xanthates.[7,20–25] The majority of these studies ignore the strong degree of coupling to be expected in the stretching modes associated with the S_2COC group. We have continued our practice of assigning the four bands as group vibrations. One of the S_2COC vibrations is shifted considerably to higher wavenumber on formation of the germyl xanthate relative to the salt and consistently appears as one of the most intense features for all compounds in the range 1205–1248 cm^{-1}. Indeed, $\nu(S_2COC)_a$ is approximately twice as intense as the peak at 1431 cm^{-1} in $Ph_3Ge[S_2CO(i\text{-}Pr)]$ and over 5 times as intense in $PhGe[S_2CO(i\text{-}Pr)]_3$. A second peak of intensity similar to that assigned to $\nu(S_2COC)_a$ appears consistently in the range 1025–1059 cm^{-1} and is assigned to $\nu(S_2COC)_c$. In most instances, the third most intense peak is in the 1086–1093-cm^{-1} region where the *q*-phenyl vibration is to be expected. In all but the isopropyl derivatives a peak in the 1086–1093 cm^{-1} is of comparable intensity to the *n*-phenyl vibration at ca. 1430 cm^{-1} and so can reasonably be assigned solely to the *q*-phenyl mode. However, in the isopropyl derivatives it is considerably more intense and so for compounds **1–3**, $\nu(S_2COC)_b$ is assumed to be coincident with the *q*-phenyl mode. For compounds **4–7**, the assignment is made to the band that has a greater intensity than can be justified on the basis of its being solely assigned to a phenyl or alkyl group vibration. Similarly, the very distinct band at ca. 660 cm^{-1} in the Raman effect of the salts is less evident in the germanium derivatives. The *v*-phenyl vibration at ca. 698 cm^{-1} is essentially not Raman active so that a band at approximately 690 cm^{-1} in the Raman effect, which increases in relative intensity along the series $Ph_3[GeS_2CO(i\text{-}Pr)]$ to $PhGe[S_2CO(i\text{-}Pr)]_3$, is clearly $\nu(S_2COC)_d$. The assignment for compounds **4–7** is more tenuous; the most intense Raman peak in the region is chosen.

(20) Watt, G. W.; McCormick, B. J. *Spectrochim. Acta* **1965**, *21*, 753.
(21) Jones, J. I.; Kynaston, W.; Hales, J. W. *J. Chem. Soc.* **1957**, 614.
(22) Andrews, D. A.; Hurtubise, F. G.; Krassig, H. *Can. J. Chem.* **1960**, *38*, 1381.
(23) Klein, E.; Bosarge, J. K.; Norman, I. *J. Phys. Chem.* **1960**, *64*, 1666.
(24) Little, L. H.; Poling, G. W.; Leja, J. *Can. J. Chem.* **1961**, *39*, 745, 1783.
(25) Shankaranarayana, M. L.; Patel, C. C. *Can. J. Chem.* **1961**, *39*, 1633.

Table XI. Mass Spectra Data of Compounds **1–5** Recorded in EI Mode[a]

ion	1	2	3	4	5
$(C_6H_5)_3Ge[S_2CO(i\text{-}C_3H_7)]^{\bullet+}$			440 (2)		
$(C_6H_5)_3Ge[S_2COC_2H_5]^{\bullet+}$					426 (4)
$C_6H_5Ge[S_2CO(i\text{-}C_3H_7)]_2^+$	421 (3)				
$(C_6H_5)_3Ge[S_2COCH_3]^{\bullet+}$				412 (2)	
$(C_6H_5)_2GeH[S_2CO(i\text{-}C_3H_7)]^{\bullet+}$		367 (7)			
$(C_6H_5)_2Ge[S_2CO(i\text{-}C_3H_7)]^+$		366 (36)			
$(C_6H_5)_3GeS^{\bullet+}$			337 (74)		337 (21)
$(C_6H_5)_2Ge[S_2COH]^+$		321 (26)			
$(C_6H_5)_3Ge^+$			305 (100)	305 (34)	305 (100)
$[S_2CO(i\text{-}C_3H_7)]_2^{\bullet+}$	270 (2)				
$HOCS_2S_2CO(i\text{-}C_3H_7)^{\bullet+}$	235 (10)				
$(C_6H_5)_2GeH^+$		229 (7)			
$(C_6H_5)_2Ge^{\bullet+}$			228 (5)		228 (4)
$(C_6H_5)(C_6H_4)Ge^+$			227 (17)		227 (8)
$C_6H_5GeS^{\bullet+}$		183 (15)	183 (9)		183 (2)
$(C_6H_5)_2^{\bullet+}$				154 (100)	154 (3)
$C_6H_5Ge^+$			153 (54)	154 (34)	153 (8)
$H_7S_2CO(i\text{-}C_3H_7)^+$	136 (78)				
$C_6H_5^+$		77 (78)	77 (11)	77 (17)	77 (5)
$C_3H_7^+$	43 (100)	43 (100)			

[a] Relative abundances are given in parentheses.

The COC deformation was identified in methylgermanium xanthates in the region 463 cm^{-1}. Thus, accidental degeneracy with the distinctive *g*-phenyl mode is to be expected, and the peak at 454–466 cm^{-1} in all compounds is broad, consistent with the presence of two peaks. In general this region is weak in the Raman effect, but in the cases of $Ph_3Ge[S_2COMe]$ and all of the isopropyl xanthates two peaks are seen in this region, split by approximately 20 cm^{-1}.

The Ge–S stretching modes are again readily identified for the isopropyl series by an increase in relative intensity of bands between 374 and 419 cm^{-1} in the Raman effect with increasing xanthate substitution. The positions of these vibrations are very similar to those of organogermanium chlorides, but these Ge–S stretches do not bring about a similar large dipole change so that the modes are only weakly infrared active.

The mass spectra were recorded for compounds **1–5** (Table XI). Very weak parent ions were observed for the triphenyl derivatives **3–5**. For **3** and **5**, the most important cluster was Ph_3Ge^+, whereas for the methyl xanthate **4** considerable rearrangement to give $Ph_2^{\bullet+}$ was apparent. The dissociation pathway clearly differed considerably for **1** and **2** with germanium-containing clusters becoming increasingly less important from mono through to tris substitution. Thus the major peaks for $PhGe[S_2CO(i\text{-}Pr)]_3$ involve the xanthate group with $C_3H_7^+$ and $H_2SCO(i\text{-}Pr)]$ being by far the most important peaks with evidence also for the formation of bis(ligand). This may be an indication why the tris species for the methyl and ethyl xanthates proved difficult to store. The crowding around germanium could bring the pendant S atoms into such close proximity that the bis(ligands) readily form and the germanium(II) species resulting from such a reductive elimination would presumably immediately react to bring about polymerization to a mixture of unidentifiable species.

Molecular Structures of $Ph_2Ge[S_2CO(i\text{-}Pr)]_2$ (2), $Ph_3Ge[S_2CO(i\text{-}Pr)]$ (3), and $Ph_3Ge[S_2COMe]$ (4). The crystal structure of diphenylbis(*O*-isopropyl dithiocarbonato)germanium (**2**) (Figure 1 and Table V) confirms that the immediate environment about germanium is the expected distorted tetrahedron. Although the bis(iso-propyl xanthate) crystallizes as orthorhombic ($P2_12_12_1$) and the bis(methyl xanthate) crystallizes as monoclinic *Cc*, the environment around germanium is essentially the same as that previously reported for diphenylbis(*O*-methyl dithiocarbonato)-germanium,[3] although the distortion from all tetrahedral angles is somewhat less. The Ge–C bond distances of 1.939 (7) and 1.927 (6) Å give an average bond length slightly longer than but comparable to those reported for $Ph_2Ge[S_2COMe]_2$ [1.918 (8) Å] or other diphenylbis(dithiocarbamates) [1.928(3) Å][11] or diphenyl bis(dithiophosphates) [1.931 (7) Å].[9]

The Ge–S bond lengths of 2.251 (3) and 2.252 (3) Å are essentially identical with those of the dithiophosphate, $Ph_2Ge[S_2P(OMe)_2]_2$ mentioned above [2.257 (2) and 2.253 (2) Å][11] and shorter than those of the methyl xanthate [2.262 (3) Å][3] or the dithiocarbamate, $Ph_2Ge[S_2CNEt_2]_2$ [2.272 (1) and 2.281 (3) Å],[11] which have the shorter Ge–C bonds. The S–Ge–S angle of 103.2 (1)° is much less distorted from the all-tetrahedral angle and opened up considerably more than in the analogous methyl xanthate where the corresponding angle is only 93.4 (2)°.[3] This is consistent with the presence of the isopropyl group preventing the xanthate groups from coming as close together as they can with only methyl substitution. The S–Ge–S angle is considerably wider than the 84.4° in $Ph_2Ge[S_2CNEt_2]_2$,[11] where the ligand is anisobidentate with the second S atom approaching the germanium atom at a distance of only 3.183 (1) Å. The angle is, however, very similar to that reported for $Ph_2Ge[S_2P(OMe)_2]_2$ of 103.4 (1)° where ligands are also essentially monodentate with the second S atom in each ligand at 5.363 (2) and 5.398 (2) Å from the germanium atom.[9] The corresponding nonbonding Ge---S distances in $Ph_2Ge[S_2CO(i\text{-}Pr)]_2$ are 4.755 (3) and 4.753 (4) Å. In the above-mentioned phosphate, the closest Ge---O distance to a methoxy group is 3.437 (1) compared to 2.981 (2) Å in $Ph_2Ge[S_2CO(i\text{-}Pr)]_2$ and 2.920 (8) Å in the bis(methyl xanthate).[3] As indicated earlier, the Ge–O interaction is proportionally much less than for the second S atom in the anisobidentate dithiocarbamate ligands, and the large differences in the C=S [1.61 (1) and 1.60 (1) Å] and C-SGe [1.75 (1) and 1.77 (1) Å] bond lengths suggest that the xanthate is essentially monodentate.[3] The

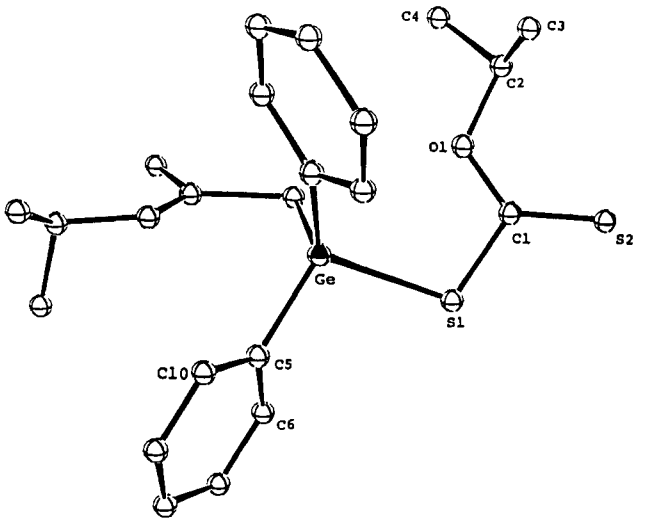

Figure 1. ORTEP plot of the molecule $Ph_2Ge[S_2CO(i\text{-}Pr)]_2$ (**2**). The atoms are drawn with 20% probability ellipsoids. Hydrogen atoms are omitted for clarity.

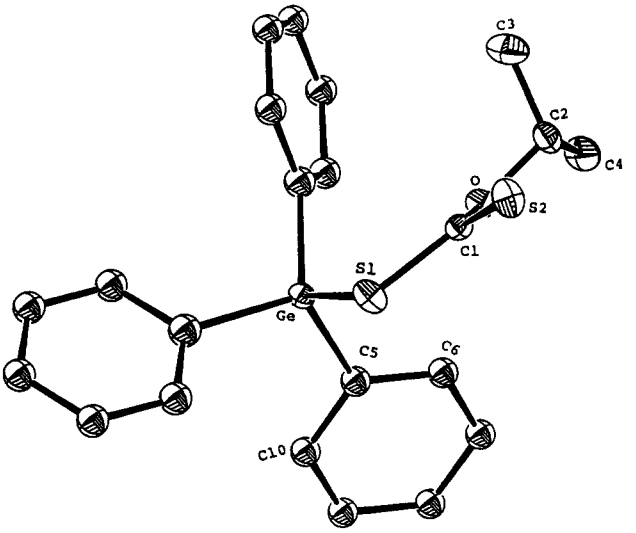

Figure 2. ORTEP plot of the molecule $Ph_3Ge[S_2CO(i\text{-}Pr)]$ (**3**). The atoms are drawn with 50% probability ellipsoids. Hydrogen atoms are omitted for clarity.

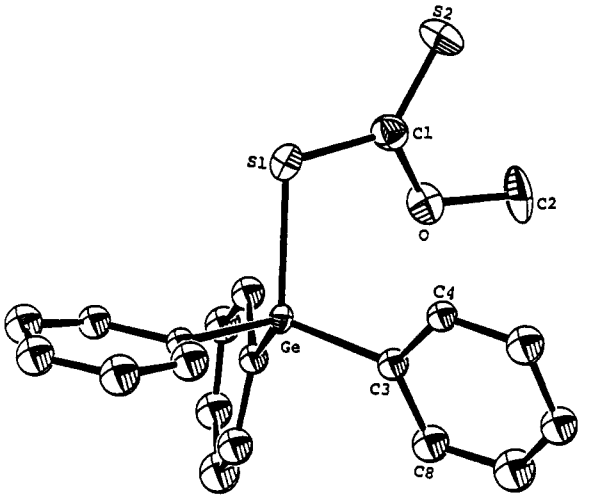

Figure 3. ORTEP plot of the molecule $Ph_3Ge[S_2COMe]$ (**4**). The atoms are drawn with 50% probability ellipsoids. Hydrogen atoms are omitted for clarity.

S_2C–O bond is also considerably shorter [1.35 (1) and 1.34 (1) Å] than the O–CR bond [1.48 (1) and 1.48 (1) Å]. Thus, there is also considerably more π-bond character in the O–CS_2 bonds than the O–CR bonds, a point to be considered relative to the shifts and changes of intensity in the IR-active stretching modes of the S_2COC group.

The crystal structures of $Ph_3Ge[S_2CO(i\text{-}Pr)]$ (**3**) (Figure 2 and Table VI) and $Ph_3Ge[S_2COMe]$ (**4**) (Figure 3 and Table VI) also show that the immediate environment about germanium is once again a distorted tetrahedron. Allowing for the fact that the structure of **3** can be resolved somewhat better than that of **4**, there appears to be no significant differences in the Ge–S and Ge–C bond lengths or S–Ge–C and C–Ge–C angles in these two monosubstituted species. The xanthate groups in both molecules are distinguished by the noninteracting S=C bond being considerably shorter, 1.629 (7) Å for **3** and 1.57 (2) Å for **4**, than the GeS—C bond, 1.729 (8) Å for **3** and 1.78 Å for **4**; the C=O bond being shorter, 1.34 (1) Å for **3** and 1.34 (2) Å for **4**, than the RC–O bond, 1.46 (1) Å for **3** and 1.44 (3) Å for **4**; the second S atom being oriented away from germanium with Ge--S distances of 4.815 (2) Å for **3** and 4.71 (1) Å for **4**; and the Ge--O distances, 3.155 (4) Å for **3** and 2.98 (1) Å for **4** being such as to preclude a significant interaction. Thus the xanthates are indeed best considered as monodentate as they are for the bis species. Therefore, neither the increased number of phenyl groups nor a change in the bulk of the R group in the xanthate appears to have any significant effect on the arrangement of groups about germanium.

It is particularly noticeable that the individual assignments of the S_2COC stretching modes, particularly for $\nu(S_2COC)_b$ and $\nu(S_2COC)_d$, differ for the methyl xanthates and their isopropyl counterparts. It would be tempting to equate the higher wavenumber for $\nu(S_2COC)_b$, 1158 cm^{-1} for **4** and **8** compared to 1086, 1085, and 1091 for **1**, **2**, and **3**, respectively, to the slightly shorter C=S bonds found for **4** of 1.57 (2) Å compared to 1.61 (1), 1.60 (1) and 1.629 (7) Å in **2** and **3** and similarly to equate the lower value for $\nu(S_2COC)_d$ of 647 and 652 cm^{-1} for **4** and **8** to the fact that the C–SGe bond appears to be slightly longer, 1.78 (2) Å. However, whether these bond length differences are significant or not, it is more probable, as mentioned earlier, that the vibrational shifts result from differences in coupling in the groups rather than small bond length changes. This is also consistent with the features being more similar for any particular xanthate, methyl, ethyl, isopropyl, or *n*-butyl, rather than relating to the number of groups present in any one molecule. In this respect, the vibrational and NMR spectra are consistent.

Acknowledgment. We wish to thank the Natural Sciences and Engineering Research Council of Canada and Imperial Oil Canada for financial support, the Ministry of Colleges and Universities of Ontario for a scholarship for M.L.Y.W., and the University of Windsor for a bursary (A.G.M.).

Supplementary Material Available: Tables SI–SIX, listing full experimental details, anisotropic thermal parameters for non-hydrogen atoms, and final fractional coordinates and thermal parameters for hydrogen atoms (9 pages); tables of observed and calculated structure factors (30 pages). Ordering information is given on any current masthead page.